

# Satellite Observations of Upper Stratospheric and Mesospheric OH: The HO<sub>x</sub> Dilemma

Robert R. Conway, Michael E. Summers<sup>1</sup> and Michael H. Stevens

E. O. Hulburt Center for Space Research, Naval Research Laboratory, Washington, DC

Joel G. Cardon

Computational Physics, Inc., Fairfax, VA

Peter Preusse and Dirk Offermann,

University of Wuppertal, Wuppertal, Germany

**Abstract.** We report the first observations of the vertical distribution of hydroxyl (OH) from the upper stratosphere to the mesopause. The Middle Atmosphere High Resolution Spectrograph Investigation (MAHRSI) made these measurements in August 1997. The data confirm the results from the earlier November 1994 MAHRSI mission that were confined to altitudes above 50 km, namely that mesospheric OH densities are 25 to 35% lower than predicted by standard photochemical theory. However, the new observations show that below 50 km the OH density increases rapidly and at 43 km altitude it is larger than that expected from standard theory. This represents a serious dilemma for our understanding of odd-hydrogen chemistry because the same key reactions are thought to dominate OH/HO<sub>2</sub> partitioning in both regions. We show that neither standard photochemical theory nor any previously proposed changes are adequate to explain the OH observations in both the upper stratosphere and mesosphere.

## 1. Introduction

It is generally believed that catalytic chemistry based upon hydrogen radicals dominates odd-oxygen (O<sub>x</sub> = O + O<sub>3</sub>) loss in the global mesosphere, whereas several catalytic cycles involving hydrogen, nitrogen, and chlorine radicals together account for the chemical loss of O<sub>x</sub> in the middle and upper stratosphere [Müller and Salawitch, 1999]. However, there are important aspects of O<sub>x</sub> chemistry, particularly of the upper stratosphere (40-50 km altitude), that remain uncertain [Osterman et al., 1997]. This is especially true of upper stratospheric odd-hydrogen (HO<sub>x</sub> = H + OH + HO<sub>2</sub>) chemistry [Jucks et al., 1998].

The ultimate source of odd-hydrogen is the photochemical destruction of H<sub>2</sub>O. This occurs mostly by photolysis above about 60 km altitude and by



<sup>1</sup>Now at the Institute for Computational Sciences and Informatics, Department of Physics and Astronomy, and Center for Earth Observing and Space Research, George Mason University, Fairfax, VA.

Copyright 2000 by the American Geophysical Union.

Paper number 2000GL011698.  
0094-8276/00/2000GL011698\$05.00

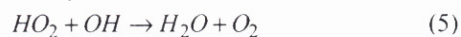
below that altitude. In the mesosphere and upper stratosphere OH/HO<sub>2</sub> partitioning is controlled by



such that

$$[OH] = \frac{k_3}{k_2} \times [HO_2] \quad (4)$$

Ultimately HO<sub>x</sub> is lost by



in these regions of the atmosphere.

The most rigorous test of standard HO<sub>x</sub> chemistry [DeMore et al., 1997] and its role in middle stratospheric O<sub>x</sub> loss has been afforded by several recent balloon-borne far-infrared experiments that measured abundance profiles for a comprehensive set of the of the key radicals and their precursor (source) molecules [Chance et al., 1996; Pickett and Peterson, 1996; Osterman et al., 1997; Jucks et al., 1998]. Most recently, Jucks et al. [1998] reported that the observed profile of the OH radical between 35-50 km altitude is consistent with that predicted by standard chemistry. Jucks et al. used model predictions of the shape of the OH height profile to extend their measurements above the 38 km balloon float height to the stratopause (~50 km). They found that their observations were best modeled by photochemical calculations incorporating a 25% reduction in the ratio of the kinetic rate coefficients of reactions (2) and (3), along with either a 25% reduction in the rate coefficient of (5) or a 25% increase in HO<sub>x</sub> production (photolysis and reaction (1)), all of which are within the quoted measurement uncertainties in DeMore et al. [1997]. Although these changes gave satisfactory agreement between model and observed OH and HO<sub>2</sub>, Jucks et al. concluded that their photochemical model underpredicted upper stratospheric O<sub>x</sub> production and thus required an additional (unknown) source of O<sub>x</sub> in the upper stratosphere in order to resolve the "ozone deficit problem".

The OH abundance at the stratopause inferred from the balloon measurements [Jucks et al., 1998] was in direct conflict with the space-based measurements of OH from the 1994 flight of the MAHRSI experiment [Conway et al., 1996; Summers et al., 1997]. MAHRSI measured OH solar

resonance fluorescence in the ultraviolet near 309 nm with high spectral resolution. Conway *et al.* [1999], hereinafter C99, give a detailed description of the experiment, the error budget, and the methods used to retrieve mesospheric OH density profiles. The 1994 MAHRSI OH data, which were restricted to the mesosphere, showed that the observed OH abundance was uniformly 25 to 35% less than the standard HO<sub>x</sub> model prediction. However, a 50% reduction (twice the quoted measurement error [DeMore *et al.*, 1997]) in the rate coefficient of reaction (3) [Clancy *et al.* 1994; Sandor and Clancy 1998], led to good agreement between model OH and the MAHRSI OH data.

Measurements of O<sub>3</sub> at the stratopause, coincident with the MAHRSI OH measurements, were made by the co-manifested CRISTA (Cryogenic Infrared Spectrographs and Telescopes for the Atmosphere) experiment [Offermann, *et al.*, 1999]. CRISTA, which was bore-sighted with MAHRSI, used three infrared telescopes and spectrometers to measure O<sub>3</sub>, several other trace gases and temperature. Taken together, the OH and O<sub>3</sub> measurements from the 1994 CRISTA/MAHRSI mission, along with the 50% change in rate constant for reaction (3), were found to nearly balance model O<sub>3</sub> production and loss at the stratopause [Summers *et al.*, 1997].

## 2. Results of the 1997 MAHRSI Mission

In August 1997 MAHRSI and CRISTA were deployed by the Space Shuttle a second time. The data from that flight provide a new perspective on the OH distribution because they include afternoon observations with solar zenith angles (SZAs) of less than 40°. These new observations provided the opportunity to extend the OH retrievals across the stratopause into the upper stratosphere. OH UV fluorescence in the upper stratosphere is difficult to measure from space because (1) the emission is absorbed by ozone, (2) the fluorescing molecules suffer efficient collisional deactivation, and (3) Rayleigh scattered sunlight that forms a spectrally complex measurement background is much brighter than in the mesosphere. All of these effects diminish the signal to noise ratio of the measured profiles. This problem was overcome for the 1997 data by averaging the spectra for each altitude

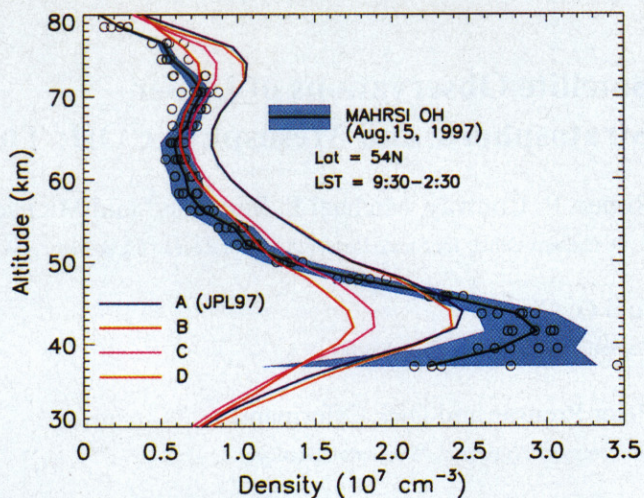


**Plate 2.** MAHRSI observations from August 15, 1997. The shaded area shows the 5-hour average of 34 limb scans for which the local time varied between 0930-1430, the solar zenith angle varied between 32-49°, and latitudes ranged between 42-58° N. The circles represent five 1-hour averaged profiles. The photochemical models are (A) Standard chemical kinetics (see text), (B) 50% reduction for reaction (2), (C) 20% reduction in rate coefficient for reaction (3) and a 30% increase for reaction (5), and (D) 25% reduction in the rate coefficients of (3) and (5). The figure shows that the shape of the observed profile is not explained by any of the models proposed for the mesosphere or the middle stratosphere.

from several limb scans. The data were binned by Solar Local Time (SLT) in five one-hour increments from 0930 to 1430 and all of these data were used to form a single profile from a grand average of 34 limb scans. Plate 1 shows the OH spectra at 50, 45.8, and 41.5 km retrieved from the grand average.

The new radiance retrievals used the O<sub>3</sub> cross-section measurements of Malicet *et al.* [1995], which have a spectral resolution comparable to MAHRSI's (0.02 nm). As described in C99, OH radiances were retrieved using a canonical background spectrum. Below about 55 km absorption by ground state OH along the MAHRSI line-of-sight caused the true background to have a slightly different shape with absorption features present at the same location as the emission lines. Correction of the OH radiances was made by an iterative adjustment of the background shape, using a high-resolution solar spectrum, high-resolution OH photoabsorption cross sections [Stevens and Conway, 1999], and forward model calculations for a range of apparent OH column densities. This led to a 7% increase in the inferred OH density at 50 km and a 19% increase at 41.5 km.

The high signal to noise ratio apparent from Plate 1 allowed the reduction of the smoothing parameter used to constrain the inversion of the intensity profiles to obtain number densities (molecules cm<sup>-3</sup>) [C99]. The reduction of both the random error and the smoothing parameter had the important effect of narrowing the inversion weighting functions shown in Figure 1. The function for a 50 km tangent height has a peak value of 0.73 at 50 km compared to a value of 0.26 for unaveraged data [C99]; the latter value implies that most of the information comes from neighboring altitudes.

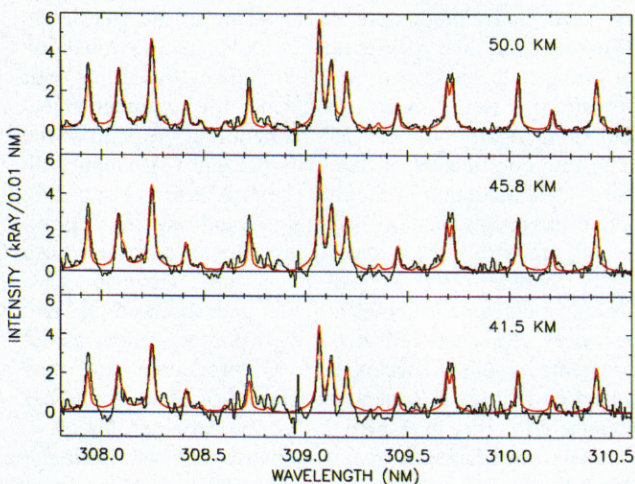


**Plate 1.** Upper stratospheric OH spectra obtained by averaging 34 limb scans (about 150 seconds of integration). Synthetic OH fluorescence spectra, scaled to fit the data, is over plotted in red for comparison.

The inversion accounts for all known processes that relate the observed intensity to the density at the line-of-sight tangent point [C99]. These include photoabsorption by upper stratospheric O<sub>3</sub> and rotational level dependent quenching of the OH A<sup>2</sup>Σ<sup>+</sup> state. The sensitivity of the upper stratosphere OH radiance retrievals to ozone variability is about three times larger than for the stratopause so that a 30% scaling of the model ozone profile used by the inversion resulted in a 30% variation in the retrieved OH density at 45.1 km. For this reason, the upper stratospheric data were inverted using a zonal average of O<sub>3</sub> observations made simultaneously by CRISTA. Comparison of the CRISTA average with a daily average O<sub>3</sub> profile from HALOE observations nearest in time and latitude showed good agreement in the critical altitude range between 40 - 47 km and at 45 km is better than 3% (0.1 PPMV). The temperature and rotational level dependence of the collisional deactivation rate coefficients for the quenching of the OH A<sup>2</sup>Σ state by N<sub>2</sub> and O<sub>2</sub> reported by Copeland et al. [1985] were fully implemented in the retrieval although no significant sensitivity was observed. We also considered vibrational energy transfer (VET) from higher lying OH vibrational levels. Williams and Crosley [1996] found that VET from the OH A<sup>2</sup>Σ<sup>+</sup> (v' = 1) level to the v'=0 level resulted in emission characterized by a high rotational temperature. Based on that report, C99 concluded that most of the VET emission was outside the MAHRSI passband so that less than 4% of the observed signal at 50 km was due to VET. For lower altitudes the contribution is further reduced due to extinction by upper stratospheric O<sub>3</sub> of the exciting solar irradiance near the OH (1,0) bandhead at 282 nm. The correction is carried as a systematic error [C99].

The MAHRSI OH density profile shown by the solid curve in Plate 2 is the result of a single inversion of the 34 co-averaged limb scans between 88-35 km as discussed above. The blue shaded region indicates the propagated measurement random error. The profile is distinguished by the rapid increase in OH below the stratopause and the well-defined stratospheric peak of  $2.9 \times 10^7 \text{ cm}^{-3}$  at 43 km. Also shown

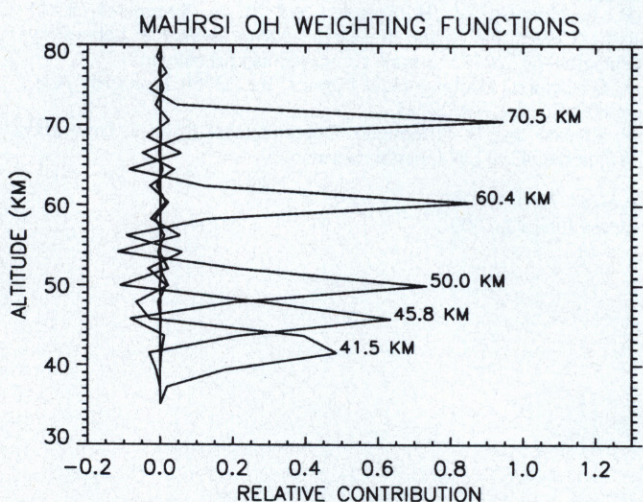


**Figure 1.** The rows of the model resolution matrix, or weighting functions, computed by the inversion of the co-averaged data. These functions indicate how the inversion smooths the "true" profile. They show that the altitude resolution of the inversion remains better than 4 km at 45.8 km.

(open circles) are the profiles for the 5 1-hour averages that are included in the grand average. These profiles lie within the measurement error of the grand average retrieval and suggest that there is little spatial and diurnal variation of OH during the 5-hour observing period.

### 3. Model/Data Comparison

The photochemical model (NRL CHEM1D) we use here is that used in our previous studies [Summers et al., 1996; Summers et al., 1997], with updated chemical kinetics and cross sections [DeMore et al., 1997]. As a validation test of the model results for the stratosphere we performed a HO<sub>x</sub> calculation for the same conditions (69° N, April 30) and model cases discussed in Jucks et al. [1998], using identical model inputs and constraints on temperature, H<sub>2</sub>O, N<sub>2</sub>O, CH<sub>4</sub>, O<sub>3</sub> and total NO<sub>y</sub> and Cl<sub>y</sub>. Our model reproduced the Jucks et al. model results for OH and HO<sub>2</sub> to better than 6%.

For this study our photochemical model was run for the same conditions as the CRISTA/MAHRSI observations (54° N, August 15). The model temperature was fixed to CRISTA observations between 20-65 km and transitioned smoothly to an MSIS climatological profile above 65 km. Model O<sub>3</sub> was fixed to the CRISTA values at 47 km and below, and transitioned to the calculated diurnally varying O<sub>3</sub> above that altitude. The model profile of H<sub>2</sub>O was obtained from a climatology of UARS Halogen Occultation Experiment (HALOE) measurements [Russell et al., 1993]. Model profiles for stratospheric CH<sub>4</sub> and N<sub>2</sub>O were obtained from CRISTA measurements, and from a HALOE climatology in the mesosphere. Model total Cl<sub>y</sub> was obtained using a climatology of HALOE HCl, and total NO<sub>y</sub> from a combination of CRISTA HNO<sub>3</sub> and a climatology of HALOE NO<sub>2</sub> and NO.

The model cases we consider follow the naming conventions of Summers et al. [1997] and Jucks et al., [1998]. Model case A uses standard chemistry, and as is seen in Plate 2 this leads to a significant overprediction of OH at all altitudes above 50 km [Summers et al., 1997]. Model B incorporates a 50% reduction in the rate coefficient of reaction (3) and yields an OH profile of approximately the same shape and magnitude as the observed OH at altitudes above 50 km. The difference between model B and data at altitudes above 70 km is due to an observed diurnal variation in the altitude of the OH peak between 70-80 km that is not reproduced in the model. We speculate this is due to the effect of a temperature tide on the OH density and will be the subject of a future report. Model case C includes a 20% reduction in (3) along with a 30% increase in (5). We cannot rule out some other combination of changes in (3) and (5) as acceptable solutions based upon analysis of mesospheric OH observations alone. Model case D incorporates a 25% reduction in both (3) and (5) [Jucks et al., 1998]. This leads to an OH profile almost indistinguishable from case A, i.e. it overpredicts OH above 50 km but underpredicts OH at the upper stratospheric peak near 43 km.

### 4. Discussion

The August 1997 MAHRSI flight confirmed that mesospheric OH abundances are lower than expected from standard HO<sub>x</sub> chemistry, just as observed during the first mission in November 1994. Given that mesospheric HO<sub>x</sub>

chemistry is thought to be relatively simple, i.e., not affected by Cl<sub>x</sub> and NO<sub>x</sub> chemistry as in the stratosphere, the implications are very clear. If standard HO<sub>x</sub> theory is complete, then one or more of the rate coefficients of the key reactions, i.e., reactions (2) and (3), controlling OH/HO<sub>2</sub> partitioning, or reaction (5), must be adjusted. Although it is possible to reproduce the observed mesospheric OH abundances with a suitable adjustment to these rate coefficients within reported uncertainties [DeMore et al., 1997], the ground based observations of lower mesospheric HO<sub>2</sub> and O<sub>3</sub> strongly favor a single reduction of a single rate coefficient of (3) [Clancy et al., 1994; Sandor and Clancy, 1998].

As seen very clearly in Plate 2, the MAHRSI results for upper stratospheric OH are in conflict with all of these model changes. The various HO<sub>x</sub> modifications shift the calculated OH profile in magnitude but leave the overall shape mostly unchanged, yet the observations show an OH scale height in the upper stratosphere that is much smaller than predicted by standard HO<sub>x</sub> chemistry and a peak density near 43 km altitude that is 20% higher. Standard chemistry does not accommodate such a dramatic change at the stratopause because the same reactions are thought to control OH/HO<sub>2</sub> partitioning in both the mesosphere and upper stratosphere. Thus we conclude that neither standard chemistry nor any of the proposed modifications is adequate to explain the observed OH vertical profile in both the upper stratosphere and mesosphere. This truly poses a dilemma for our understanding of HO<sub>x</sub> chemistry in the middle atmosphere. Furthermore, the shape of that profile has important and as yet unquantified implications for the analyses of the balloon-borne observations that extended their results upward to the stratopause by assuming that the shape of the OH profile in the upper stratosphere is essentially that predicted by standard HO<sub>x</sub> chemistry.

**Acknowledgments.** We thank Ken Jucks for providing the FIRS-2 data and for supplying observational constraints for their photochemical model calculation at 69° N. The Office of Naval Research, the NASA Offices of Earth Science and Space Science, and DARA/DLR (Bonn) supported this work.

## References

- Chance, K., et al., Simultaneous measurements of stratospheric HO<sub>x</sub>, NO<sub>x</sub> and Cl<sub>x</sub>: Comparison with a photochemical model, *J. Geophys. Res.*, **101**, 9031-9043, 1996.
- Clancy, R.T., B.J. Sandor, and D.W. Rusch, Microwave observations and modeling of O<sub>3</sub>, H<sub>2</sub>O, and HO<sub>2</sub> in the mesosphere, *J. Geophys. Res.*, **99**, 5465-5473, 1994.

- Conway, R. R., et al., Satellite measurements of hydroxyl in the mesosphere, *Geophys. Res. Lett.*, **23**, 2093-2096, 1996.
- Conway, R. R., et al., The Middle Atmosphere High Resolution Spectrograph Investigations, *J. Geophys. Res.*, **104**, 16,327-16,348, 1999.
- Copeland, R.A. M.J. Dyer, and D.R. Crosley, Rotational-level-dependent quenching of A<sup>2</sup>Σ<sup>+</sup> OH and OD, *J. Chem. Phys.*, **82**, 4022-4032, 1985.
- DeMore, et al., Chemical Kinetics and Photochemical Data for Use in Stratospheric Modeling, Evaluation No. 12, *Publ. 97-4*, Jet Propulsion Laboratory, Pasadena, CA, 1997.
- Jucks, K.W. et al., Observations of OH, HO<sub>2</sub>, H<sub>2</sub>O, and O<sub>3</sub> in the upper stratosphere: Implications for HO<sub>x</sub> photochemistry, *Geophys. Res. Lett.*, **25**, 3935-3938, 1998.
- Malicet, J. et al., Ozone UV Spectroscopy. II. Absorption Cross-Sections and Temperature Dependence, *J. Atmos. Chem.*, **21**, 263-273, 1995.
- Müller, R., and R.J. Salawitch, Upper Stratospheric Processes, Chapter 6, Scientific Assessment of Ozone Depletion: 1998, *World Meteorological Organization - Report No. 44*, 1999.
- Offermann, D., et al., Cryogenic Infrared Spectrometers and Telescopes for the Atmosphere (CRISTA) experiment and middle atmospheric variability, *J. Geophys. Res.*, **104**, 16311-16326, 1999.
- Osterman, G.B., et al., Balloon-borne measurements of stratospheric radicals and their precursors: Implications for the production and loss of ozone, *Geophys. Res. Lett.*, **24**, 1107-1110, 1997.
- Pickett, H.M. and D.B. Peterson, Comparison of measured stratospheric OH with prediction, *J. Geophys. Res.*, **101**, 16,789-16,796, 1996.
- Russell, J.M., et al., The Halogen Occultation Experiment, *J. Geophys. Res.*, **98**, 10777-10797, 1993.
- Sandor, B.J. and R.T. Clancy, Mesospheric HO<sub>x</sub> chemistry from diurnal microwave observations of HO<sub>2</sub>, O<sub>3</sub>, and H<sub>2</sub>O, *J. Geophys. Res.*, **103**, 13337-13352, 1998.
- Stevens, M.H. and R.R. Conway, Calculated OH A<sup>2</sup>Σ<sup>+</sup>-X<sup>2</sup>Π (0,0) band rotational emission rate factors for solar resonance fluorescence, *J. Geophys. Res.*, **104**, 16369-16378, 1999.
- Summers, M.E., et al., Mesospheric HO<sub>x</sub> Photochemistry: Constraints from concurrent measurements of OH, H<sub>2</sub>O, and O<sub>3</sub>, *Geophys. Res. Lett.*, **23**, 2097-2100, 1996.
- Summers, M.E., et al., Implications of Satellite OH Observations for Middle Atmospheric H<sub>2</sub>O and Ozone, *Science*, **277**, 1967-1970, 1997.
- Williams, L.R. and D.R. Crosley, Collisional vibrational energy transfer of OH(A<sup>2</sup>Σ<sup>+</sup>, v=1), *J. Chem. Phys.*, **104**, 6507, 1996.

R. R. Conway, M. H. Stevens, and M. E. Summers\*, E. O. Hulburt Center for Space Research, Naval Research Laboratory, Washington, DC 20375 (e-mail: conway@map.nrl.navy.mil)  
 J. G. Cardon, Computational Physics, Inc., 2750 Prosperity Ave., Suite 600, Fairfax, VA 22031  
 P. Preusse and D. Offermann, Department of Physics, University of Wuppertal, 42097 Wuppertal, Germany.

(Received April 19, 2000;  
 accepted June 12, 2000.)